Hydrogen Bonding in 2-Propanol. The Effect of Fluorination†

Holger Schaal, Thomas Häber, and Martin A. Suhm*

Institut für Physikalische Chemie, Universität Göttingen, Tammannstrasse 6, 37077 Göttingen, Germany

Received: August 12, 1999

Fourier transform infrared (FTIR) spectra at thermal equilibrium and in seeded, pulsed slit jet expansions of 2-propanol (IP), 1,1,1-trifluoro-2-propanol (TFIP), and 1,1,1,3,3,3-hexafluoro-2-propanol (HFIP) reveal dimers, oligomers, and large clusters as well as conformational isomerism of the monomers. The assignments are supported by hybrid density functional calculations. The effect of methyl group fluorination on OH frequency shift and intensity enhancement, torsional energetics, hydrogen bond strength, and cluster stability trends is investigated. HFIP promises to be a valuable prototype for spectroscopic studies of intramolecular torsional isomerization dynamics (as already shown in Quack, M. *Faraday Discuss. Chem. Soc.* **1995**, *102*, 104−107) and its coupling to intermolecular hydrogen bonding.

1. Introduction

Fluorinated methyl groups are frequently used to tailor the properties of pharmacologically active compounds.[1] Hydroxylic hydrogen bond interaction is a major mechanism in biochemical activity. Therefore, a quantitative study of the effect of fluorination on hydrogen bonding in simple, prototypical alcohols may provide insights into some effects observed in drug design. We have studied 2-propanol (isopropanol, IP) and its tri- and hexafluorinated derivatives 1,1,1-trifluoro-2-propanol (TFIP) and 1,1,1,3,3,3-hexafluoro-2-propanol (HFIP) as well as their hydrogen-bonded clusters in our first effort toward this goal. TFIP is attractive due to its chiral structure, which leads to intermolecular, hydrogen bond induced diastereoisomerism with distinct spectral features. HFIP is a powerful solvent for β-sheet aggregated peptides[2] and a fragment of interesting fluorinated alcohols[3] and anesthetics.[4]

TFIP and HFIP have repeatedly been studied by conventional IR and Raman techniques since the late 1960s.[5−13] In the gas phase, HFIP occurs in two spectrally and energetically well separated conformations[7,12,13] due to interactions of the hydroxyl group with the CF_3 substituents. There is considerable debate on whether this interaction is of the hydrogen bond type.[3,14−16] Sum and difference bands related to OH torsion and other low-frequency fundamentals are relatively strong. The intramolecular stabilization of the C_S conformer is reduced in CCl_4 solutions.[5,6] In the neat liquid phase at room temperature, OH-stretching bands corresponding to "free" OH groups persist as shoulders on a broad associated OH band, whereas the conformational splitting in the CH-stretching region disappears.[6] In the solid phase, pronounced association bands emerge in the CH-stretching region.[7] They are probably due to overtone and combination bands which steal intensity from the associated OH stretching fundamental. This rich spectral signature of isomerism and phase state makes HFIP well suited for a detailed cluster investigation, which we initiate in this paper. Conformational isomerism in TFIP[9,11] is less clear-cut in the infrared spectrum of the gas phase, and the association phenomena are complicated by the presence of two enantiomers. Due to its bridging function between IP and HFIP and in preparation for a study of the enantiomerically pure compound, we have also investigated the infrared spectrum of racemic TFIP.

Our investigation starts with a refined IR gas-phase investigation of IP and its fluorinated derivatives, which leads to the assignment of dimer association bands in all three cases. To characterize the dimers and larger oligomers in more detail, supersonic jet experiments[17] using a new, sensitive direct absorption technique[18−20] are carried out. The assignment of the spectra is supported by exploratory electronic structure calculations using a hybrid density functional. Larger clusters are generated as well and their absorptions can be compared to spectra of the liquid and solid phases.

2. Experimental Section

Infrared spectra were recorded with our Bruker IFS 66v/S spectrometer (maximum resolution 0.1 cm^{-1}) equipped with CaF_2 and KBr beam splitters and optics as well as InSb, HgCdTe, and DTGS detectors. For weak absorptions in the OH stretching region, an optical filter (2.5−3.5 μm, OCLI) was used. Care was taken to avoid saturation and the resulting nonlinearities in the cooled detectors. Band integrations were carried out by using the OPUS software (Bruker), employing method A (integrating from the baseline) or B (above a line joining the spectral values at the borders of the integration interval), as appropriate. The estimated absolute error for integrated intensities is ±20% or ±2 km/mol, whichever is larger.

Gas spectra were recorded at room temperature (298 ± 5 K) in a 222.8 mm glass cell (Bruker) equipped with CaF_2 windows. Reference spectra of the liquid alcohols at room temperature were obtained in transmission (using a film between sealed CaF_2 windows) and via attenuated total reflection (ATR) using a single reflection at a ZnSe/liquid interface (Specac).

Spectra of cooled monomers and clusters were obtained in a high throughput supersonic jet expansion synchronized to rapid mirror scans. Details of the setup are given elsewhere.[20] Briefly, we expand a gas mixture of the alcohol and a carrier gas (He, 99.996% and Ar, 99.998%, Messer-Griesheim) from a 0.065 m^3 gas buffer through a pneumatically operated, pulsed slit nozzle (Parker, Series 97) of dimensions 120 × 0.6 mm into a

† Dedicated to Prof. Dr. W. Lüttke on the occasion of his 80th birthday.

* Corresponding author. E-mail: msuhm@gwdg.de/FAX: +49 551 393117.

10.1021/jp9928558 CCC: $19.00
Published on Web 12/16/1999

7 m^3 vacuum buffer chamber pumped by a series of roots pumps. The pulse duration ranges from 70 to 500 ms and is synchronized to a sequence of one to seven full rapid FTIR scans. Compared to continuously operated slit jet FTIR setups,[21,22] much larger slit dimensions and throughputs can be realized.[17,23] The background pressure at the end of the pulse remains well below 1 mbar. The mixture is prepared by bubbling the carrier gas through thermostated saturator chambers filled with the liquid alcohol. The concentration is adjusted via temperature control of the saturator and by admixture of pure carrier gas to the 0.065 m^3 chamber. The jet expansion is sampled by the collimated IR beam from an external spectrometer port. For optimal dimer absorptions, a circular 5-mm diameter section or a square 10-mm section which partly overlaps the nozzle throat is extracted by an aperture.

2-Propanol (IP, 99.5%, Fluka) and 1,1,1,3,3,3-hexafluoro-2-propanol (HFIP, 99%, Fluka) were used as supplied, whereas 1,1,1-trifluoro-2-propanol (TFIP, racemic, 97%, Lancaster) was desiccated by using 3-Å molecular sieve (Roth) prior to use. The alcohols were freed of dissolved gases by repeated freeze−pump−thaw cycles. Vapor pressures at the employed saturator temperatures were taken from the literature,[24] combined with extrapolation based on the enthalpy of vaporization. The fluorinated alcohols, in particular HFIP, have a considerable tendency to swell elastomer O-rings, but Viton proved to be sufficiently inert.

3. Notation and Modeling of Conformational Isomerism

To support the vibrational and size assignment in the supersonic jet spectra, exploratory hybrid density functional calculations using the B3LYP functional and a 6-31+G* basis set were applied to monomers, dimers, and trimers of IP, TFIP, and HFIP, using the Gaussian94 and Gaussian98 program packages.[25] This approach is known to perform reasonably well for hydrogen bonds and in particular for hydrogen bond induced wavenumber shifts, also including fluorine.[26] Ultimately, a local MP2 approach[27] would be preferable, also because it eliminates correlation contributions to the basis set superposition error. We compare harmonic predictions of wavenumber shifts without correction for basis set superposition error to fully anharmonic wavenumber shifts from experiment. While this approach relies on substantial error cancellation,[28] it provides us with a very useful assignment aid. Infrared band strengths are estimated within the double-harmonic approximation.[29] They turn out to be useful for the evaluation of dimerization and isomerization equilibria based on experimental intensity data, although B3LYP infrared intensities must generally be viewed with some caution. The use of free energy predictions based on harmonic oscillator/rigid rotor models is less robust and at best qualitative due to the presence of floppy low-frequency modes.

The molecules and clusters involved in this study contain several torsional degrees of freedom, which we classify according to the torsional angle and its associated sequence rules.[30] For the internal torsion of the symmetric 2-propanols (IP and HFIP), the torsion angle H−C−O−H is given and local minima have the two end atoms either (±sc) (synclinal, around ±60°) or (ap) (antiperiplanar, around 180°) to each other. For TFIP, the torsion angle CF_3−C−O− H is indicated as (+sc), (−sc), or (ap), in addition to the absolute configuration (*R*,*S*) at the central carbon atom. A hydrogen bond between two monomers forms a new stereogenic center, but we prefer to classify it as a new torsional degree of freedom of the acceptor molecule, i.e., H−C−O···H, while we do not specify the very floppy torsion of the donor molecule explicitly.

TABLE 1: Monomer Properties for 2-Propanol (IP)[a]

	(±sc)-IP	(ap)-IP	source
$\tilde{\nu}_{OH}/cm^{-1}$	3658	3636 ⟨22⟩	cell,[b] jet
ω/cm^{-1}	3831(5)	3805(6) ⟨26⟩	experiment[32]
$\omega_{OH}^{B3LYP}/cm^{-1}$	3744	3724 ⟨20⟩	6-31+G*
$\bar{A}_{OH}^{exp}/(km\ mol^{-1})$	13 (total)		cell
$\bar{A}_{OH}^{B3LYP}/(km\ mol^{-1})$	13	11	6-31+G*
$\bar{A}_{OH}^{MP2}/(km\ mol^{-1})$	12	11	6-311+G*
$\bar{A}_{CH}^{exp}/(km\ mol^{-1})$	25 (total)		cell
$\bar{A}_{CH}^{B3LYP}/(km\ mol^{-1})$	33	28	6-31+G*
$\bar{A}_{CH}^{MP2}/(km\ mol^{-1})$	25	21	6-311+G*
$\Delta E_h^{B3LYP}/(kJ\ mol^{-1})$		⟨−0.8⟩	6-31+G*

[a] Values in brackets correspond to the difference between (sc) and (ap) conformers. $\tilde{\nu}$ and ω are anharmonic and harmonic band centers, $\bar{A}$ denotes integrated absorption coefficients, which are normalized by the number of C−H bonds in the CH case. ΔE_h^{B3LYP} is the difference in energy between the conformers at 0 K, including harmonic zero point energy contributions. [b] Within 1 cm^{-1} of a previous band center determination.[32]

Our stereochemical notation thus consists of a sequence of torsion angle specifications for the donor (D), acceptor (A), and hydrogen-bond (H) conformations, such as in $(ap)^D(ap)^A(\pm sc)^H$−HFIP, an enantiomeric pair of dimers formed from two HFIP monomers in their (ap) conformation (see Figure 6 for its structure).

4. Monomer Isomerism

Prior to a study of hydrogen bond association, the monomer spectra have to be analyzed in the OH and CH stretching region. The OH stretching band of IP reveals at least two overlapping bands separated by 22 cm^{-1} (see Table 1 and Figure 1). The dominant, high-frequency component exhibits a Q-branch doublet.[31] This band has been assigned before to the (±sc) or gauche conformer.[31,32] Relative energies and relative harmonic frequencies from our B3LYP calculation (Table 1) fully support this assignment. The absolute harmonic wavenumbers are underestimated by 2% and therefore fall midway between experimental anharmonic and experimental harmonic wavenumbers. The latter were obtained from an analysis of the overtone spectrum.[32] As usual, wavenumber differences are much more reliable in absolute terms, due to systematic error compensation. Comparison to rotationally cold supersonic jet spectra (see below) proves that the high-frequency band belongs to the stable conformer. Its band center does not show a significant temperature dependence. The experimental OH band strength of 13 km/mol (Table 1) is in line with the average value of 13.8 ± 0.4 km/mol found for secondary alcohols in CCl_4 solution,[33] although the specific value determined for IP, 14.3 km/mol,[33] hints at a slight intensity enhancement[34] or conformational shift induced by the solvent. Integrated band strengths from the B3LYP calculation are in good agreement with experiment for the OH stretching band, whereas the average CH band strength per CH bond is somewhat overestimated. MP2 calculations yield similar OH band strengths, but only when triple-ζ basis sets are employed (Table 1). In contrast, MP2 band strengths for the CH chromophore are in somewhat better agreement with experiment than the B3LYP results.

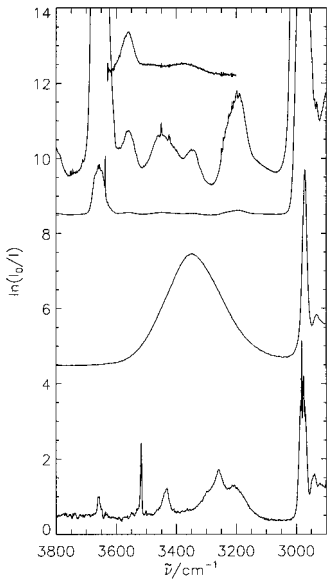

Figure 1. OH/CH stretching spectra of IP ($p = 49.4$ mbar) in the gas phase (top three traces, from bottom to top: regular spectrum; regular spectrum multiplied by 20; cluster fraction after subtraction of the monomer contribution, multiplied by 20), in the liquid phase (next lower trace, liquid film, recorded in transmission, multiplied by 8), and in the supersonic jet (lowest trace, multiplied by 1500, conditions: 0.2% in He, stagnation pressure of 0.6 bar, resolution 2 cm^{-1}).

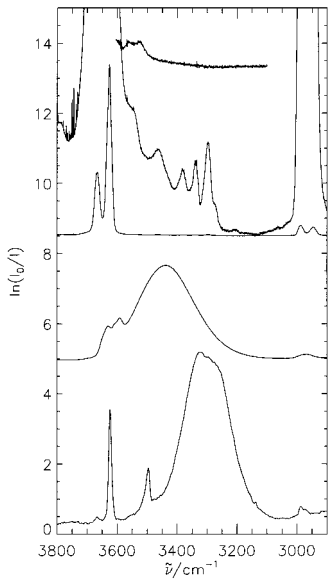

Figure 2. OH/CH stretching spectra of HFIP ($p = 29.4$ mbar) in the gas phase (top three traces, from bottom to top: regular spectrum; regular spectrum multiplied by 80; cluster fraction after subtraction of the monomer contribution, multiplied by 80), in the liquid phase (next lower trace, liquid film, recorded in transmission, multiplied by 1.5), and in the supersonic jet (lowest trace, multiplied by 190, ≈1% in He, stagnation pressure between 0.4 and 1 bar, resolution 4 cm^{-1}).

TABLE 2: Monomer Properties for 1,1,1,3,3,3-Hexafluoro-2-propanol (HFIP)[a]

	(±sc)-HFIP	(ap)-HFIP	source
$\tilde{\nu}_{OH}$/cm^{-1}	3667	3626	cell[b]
		⟨41⟩	
$\tilde{\nu}_{OH}$/cm^{-1}	3667	3624	jet
		⟨43⟩	
ω_{OH}^{B3LYP}/cm^{-1}	3759	3718	6-31+G*
		⟨41⟩	
$\bar{A}_{OH}^{exp}$/(km mol^{-1})	54 (total)		cell
$\bar{A}_{OH}^{B3LYP}$/(km mol^{-1})	69	57	6-31+G*
$\tilde{\nu}_{CH}$/cm^{-1}	2946	2988	cell[b]
		⟨−42⟩	
ω_{CH}^{B3LYP}/cm^{-1}	3060	3129	6-31+G*
		⟨−69⟩	
$\bar{A}_{CH}^{exp}$/(km mol^{-1})	5 (total)		cell
$\bar{A}_{CH}^{B3LYP}$/(km mol^{-1})	11	3	6-31+G*
ΔE_{min}^{B3LYP}/(kJ mol^{-1})		⟨5.2⟩	6-31+G*
ΔE_{h}^{B3LYP}/(kJ mol^{-1})		⟨4.5⟩	6-31+G*

[a] Values in brackets correspond to the difference between (sc) and (ap) conformers. $\tilde{\nu}$ and ω are anharmonic and harmonic band centers, $\bar{A}$ denotes integrated absorption coefficients. ΔE_h^{B3LYP} (ΔE_{min}^{B3LYP}) is the difference in energy between the conformers at 0 K including (excluding) harmonic zero point energy contributions. [b] Within 1 cm^{-1} of a previous band center determination.[12]

In the case of HFIP (Table 2, Figure 2), two bands separated by 41 cm^{-1} are found in the OH stretching region. The higher frequency band also exhibits a double peak structure, but in contrast to IP, the doublet is less pronounced and the low-frequency band is now stronger than the doublet bands. This low-frequency band has been assigned to the (ap) HFIP conformation before.[7,10,12,13] Our B3LYP results for the stretching frequency support this assignment and reproduce the wavenumber difference between the two isomers quantitatively. Upon cooling in the supersonic jet, the low-frequency band dominates the spectrum. This confirms previous findings[7,10,12,13] that the (ap) conformer is lower in energy. A slight shift of the band maximum to lower wavenumber upon cooling may indicate additional complexity in this band, in support of earlier findings.[7] Based on the approximate B3LYP integrated band strength ratio, an equilibrium constant $K_p = p_{(\pm sc)}/p_{(ap)} \approx 0.4(1)$ at 298 K can be estimated from the experimental band intensities of the two OH stretching bands. The predicted total integrated absorption intensity of 60 km/mol is in good agreement with the experimental value of 54 km/mol. This corresponds to a 4-fold enhancement compared to the value for aliphatic alcohols in general[33] and 2-propanol in particular. One possible explanation for this enhancement is the formation of intramolecular hydrogen bonds to the fluorine atoms, which has also been invoked to explain the enhanced stability of the (ap) conformer.[5] However, other influences of the polar C−F bonds are also conceivable.

A similar analysis can be carried out for the CH-region, where two weak bands separated by 42 cm^{-1} can be found. On the basis of relative intensities, the higher frequency band can be assigned to the (ap) conformer. Using the approximate B3LYP integrated band strength ratio, $K_p \approx 0.25(10)$ is derived at 298 K in rough agreement with the OH result. The predicted integrated absorption intensity for this conformer ratio is 4 km/mol, in good agreement with the observed value of 5 km/mol.

The B3LYP calculation itself predicts $K_p = 0.26$ within a simple harmonic oscillator/rigid rotor model, after inclusion of the proper degeneracy factor in the (±sc) partition function. Previous rough estimates building on the temperature dependence of the OH ($K_p = 0.46$) and CH ($K_p = 0.26$) Raman bands without consideration of different scattering intensities for the two conformers[12] are also consistent with these results. The B3LYP enthalpy difference $\Delta H_{298}^{\circ} = 4.7$ kJ/mol is in good agreement with the experimental values of 4.0(1.6) kJ/mol and 6.0(2.8) kJ/mol.[12] In CCl_4 solution, this energy difference is reduced by 1 order of magnitude.[5] The harmonic B3LYP energy difference at the zero-point level (4.5 kJ/mol, Table 2) agrees well with an early experimental estimate (ca. 4±1 kJ/mol[10]),

TABLE 3: Monomer Properties for 1,1,1-Trifluoro-2-propanol (TFIP)[a]

	(+sc)-*R*	(−sc)-*R*	(ap)-*R*	source
$\tilde{\nu}_{OH}/cm^{-1}$	3653	3637		cell[b]
		⟨16⟩		
$\omega_{OH}^{B3LYP}/cm^{-1}$	3744	3729	3763	6-31+G*
		⟨15⟩	⟨−19⟩	
$\bar{A}_{OH}^{exp}/(km\ mol^{-1})$		33 (total)		cell
$\bar{A}_{OH}^{B3LYP}/(km\ mol^{-1})$	38	30	35	6-31+G*
$\bar{A}_{CH}^{exp}/(km\ mol^{-1})$		14 (total)		cell
$\bar{A}_{CH}^{B3LYP}/(km\ mol^{-1})$	16	12	19	6-31+G*
$\Delta E_{min}^{B3LYP}/(kJ\ mol^{-1})$		⟨−2.5⟩	⟨−11.0⟩	6-31+G*
$\Delta E_{h}^{B3LYP}/(kJ\ mol^{-1})$		⟨−2.3⟩	⟨−9.4⟩	6-31+G*

[a] Values in brackets give the difference from the (+sc)-R result. $\tilde{\nu}$ and ω are anharmonic and harmonic band centers, $\bar{A}$ denotes integrated absorption coefficients, which are normalized by the number of C−H bonds in the CH case. ΔE_h^{B3LYP} (ΔE_{min}^{B3LYP}) is the difference in energy between the conformers at 0 K including (excluding) harmonic zero point energy contributions. [b] Within 1 cm^{-1} of a previous band center determination.[11]

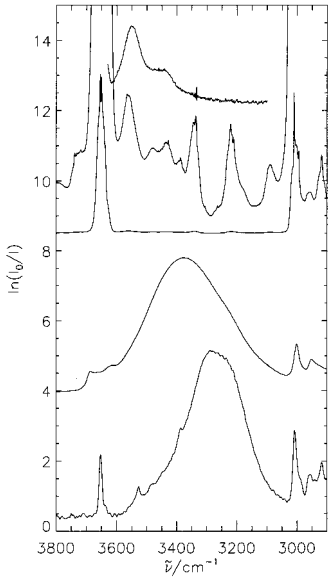

Figure 3. OH/CH stretching spectra of TFIP (p = 45 mbar) in the gas phase (top three traces, from bottom to top: regular spectrum; regular spectrum multiplied by 50; cluster fraction after subtraction of the monomer contribution, multiplied by 50), in the liquid phase (next lower trace, liquid film, recorded in transmission, multiplied by 8), and in the supersonic jet (lowest trace, multiplied by 400, ≈0.5% in He, stagnation pressure 0.8 bar, resolution 4 cm^{-1}).

which was published in 1995.[13] Even the barrier height for isomerization (≈10 kJ/mol) agrees well with an elegant, if oversimplified, experimental estimate.[35] However, in the case of barriers, like in the case of infrared intensities, particular caution is indicated when interpreting density functional results.

The OH stretching spectrum of TFIP is quite similar to that of IP with a split high-frequency band and a weaker band on the low-frequency shoulder (Table 3 and Figure 3). Murto et al.[9] assign the dominant band to the (+sc)-*R* or (−sc)-*S* conformer. This assignment has been challenged by Durig et al.[11] on the basis of band shape simulations. Durig et al. assign the strongest band to the (ap) conformer. The B3LYP results strongly favor the earlier (+sc)-*R*/(−sc)-*S* assignment,[9] based on relative energy and fundamental wavenumber. MP2 calculations using a larger basis set confirm this conclusion. The (ap) conformer is predicted to be 11 kJ/mol higher in energy than the (+sc)-*R*/(−sc)-*S* structure. Its predicted harmonic wavenumber is 110 cm^{-1} higher than the dominant experimental band center, whereas all other OH-stretch predictions of IP, TFIP, and HFIP are 86−92 cm^{-1} above the experimental bands. Moreover, the predicted wavenumber shift between the two lowest conformations is 15 cm^{-1}, in agreement with experiment (16 cm^{-1}), whereas the two lowest conformers according to Durig et al. are predicted to be 34 cm^{-1} apart. The presence of a characteristic doublet in the (+sc)-*R*/(−sc)-*S* band of TFIP as in IP and HFIP undermines its proposed interpretation as a (tunneling) split ground level,[31] as there are no equivalent torsional minima in TFIP. The predicted integrated absorption intensity for the TFIP OH bands (30−38 km/mol, depending on the conformation) agrees well with the experimental value of 33 km/mol, which is exactly midway between those of IP and HFIP. The weak dependence of this band strength on conformation suggests that the fluorine-induced enhancement is not dominated by the formation of intramolecular hydrogen bonds. The observed integrated absorption intensity of the CH stretching manifold (14 km/mol per CH bond) falls in the range of values predicted for the various conformers (12−19 km/mol). Our jet spectra (Figure 3) support the assignment of the high-frequency band to the low-energy conformer.

Figure 4 compares the OH torsional potentials for the three alcohols at B3LYP 6-31+G* level with full relaxation of all other degrees of freedom. For IP (upper trace in Figures 4a,b), there are only minor energy differences between the (± sc) and (ap) wells. The TFIP conformation with the same local OH environment as in (± sc)-IP corresponds to a very shallow well (middle trace in Figure 4b). This indicates that the effect of the remote CF_3 group is substantial. Conformations in which the OH group is adjacent to the CF_3 group are energetically much more favorable and form deep wells. The deepest of these wells provides the same local environment to the OH group as the (±sc)-HFIP conformation. However, the latter is more shallow, which is another indication of the destabilizing effect of a trans-CF_3 group. The (ap) conformation of HFIP, which avoids a trans-CF_3 group to the OH bond, has a stability comparable to that of the most stable TFIP conformation.

In summary, the OH group in the investigated compounds prefers a staggered position where the neighborhood to CF_3 groups is maximized, while the interaction with CH_3 groups is minimized. An (ap) arrangement of CF_3 and OH groups is strongly disfavored. The simple harmonic B3LYP 6-31+G* calculations are in remarkable agreement with experimental data for IP, TFIP, and HFIP. While part of this agreement is due to systematic error cancellation, it provides a good basis for the estimation of dimer and trimer spectra of these compounds, which will be compared to experiment in the following sections.

5. Hydrogen Bonding in the Vapor Phase

The study of dimers and oligomers of alcohols at ambient temperatures has a long tradition.[36−39] By dilution in more or less inert solvents such as CCl_4, a wide range of monomer concentration can be realized. Quantitative determination of the monomer band depletion leads to dimerization constants:

$$K_{c,2} = c_D/c_M^2$$

For aliphatic alcohols, $K_{c,2}$ is found to depend only weakly on the nature and size of the alkyl group.[39]

However, several problems exist for such an approach. The solubility can be small. Solvent effects can be sizable[6] and may even suppress dimerization at high dilution.[40] Absorption bands

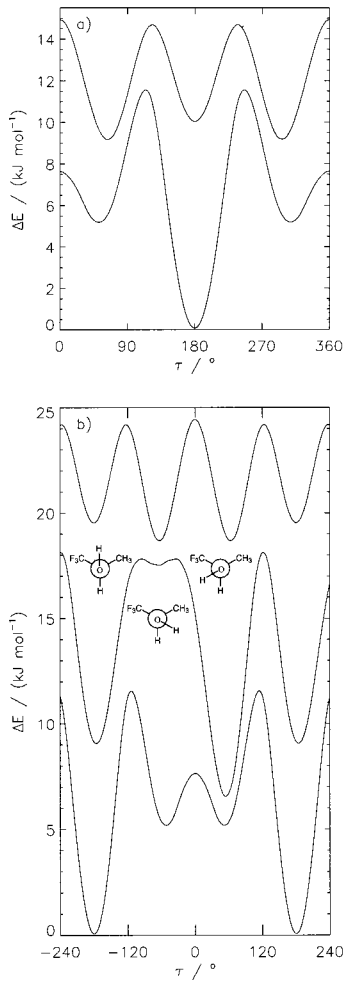

Figure 4. OH torsional potentials for (a) the symmetric alcohols IP (upper) and HFIP (lower trace) from 0 to 360° and (b) all three alcohols IP (upper), TFIP (middle), and HFIP (lower trace) from −240° to 240° for better comparability. In both figures, the relative electronic stability of the monomer conformations at the B3LYP 6-31+G* level is plotted as a function of the OH torsional angle τ relative to the secondary CH bond. All other degrees of freedom are optimized along the path. In (b), the three potential curves are drawn on the same energy scale and shifted into close contact for conformations with similar local environment. From left to right, minima corresponding to trans, gauche, gauche and trans conformations of the two H-atoms are drawn, as indicated explicitely for TFIP.

due to non-hydrogen-bonded OH end groups fall in the range of monomeric OH absorptions and may mask its concentration dependence. Therefore, it is desirable to have gas-phase dimerization results for comparison.[8] Competition from bulk condensation usually prevents the formation of large amounts of dimers or higher oligomers in the gas phase. Condensation is favored over gas-phase clustering due to dispersion forces and other 3-D attractive, more or less isotropic interactions.[18] Therefore, methanol exhibits more pronounced vapor phase association than larger, more polarizable alcohols. Alkyl group fluorination generally increases the volatility of alcohols.[24]

The determination of dimerization constants ($p^{\ominus} = 1$ bar)

$$K_{p,2} = p_D p^{\ominus}/p_M^2$$

in the gas phase is less straightforward than in solution. Monomer depletion is often too small to be measured reliably. Instead, a theoretical estimate for the dimer OH band strength can be used. In the dimer, the donor OH stretching intensity is strongly enhanced with respect to that of the monomer. This enhancement is quite sensitive to excitation of the hydrogen bond, i.e., to temperature. The double-harmonic estimate obtained from the B3LYP calculation is very likely an overestimate for the band strength at 298 K, since it does not include zero-point or thermal averaging effects, which weaken the hydrogen bond. From the liquid-state results of Finch and Lippincott,[41] an overestimation by a factor of 2−3 is quite likely.

A second difficulty concerns the identification and isolation of the dimer OH absorption from monomer bands. This is achieved by variation of the pressure. Bands varying more than linearly with pressure are due to dimers or larger oligomers. A corresponding band has been identified in the gas phase for IP.[8] For TFIP and HFIP, evidence for such bands has so far only been circumstantial[6,9] and in some cases restricted to spectra recorded in CCl_4 solutions. To characterize the dimer OH stretching region more accurately, we have employed a simple spectral subtraction scheme which is based on the strong intensity enhancement upon dimerization. Gas-phase absorbance spectra S_p and $S_{p'}$ recorded at different pressures ($p > p'$) are normalized by division through the corresponding pressure and then subtracted from each other. The resulting spectrum is multiplied by $p''/(p - p')$ to approximate a pressure-normalized dimer spectrum S_D at pressure p'' ($p' > p''$) nearly without monomer contributions. This dimer spectrum is subtracted from a measured gas-phase spectrum at p'', thus providing a pure monomer spectrum at p'', which can in turn be subtracted from the series of experimental pressure-normalized spectra. The resulting difference spectra can now be integrated and identified as dimer bands via a linear variation of the band strength with pressure.

The top trace of Figures 1−3 shows spectra for which the regular monomer contributions have been removed in this way. For IP, a well-defined band is seen at 3562(2) cm^{-1}, 104 cm^{-1} below the dominant monomer band. It can be assigned to the hydrogen bond donor OH stretching fundamental. Much weaker bands near 3480 and 3375 cm^{-1} may be due to trimer and tetramer species, as we will see below. In the case of HFIP (Figure 2), a weak doublet at 3562(4) and 3527(2) cm^{-1} is superimposed on a pronounced slope. The slope may arise from pressure-dependent collision-induced absorptions in this polar gas or from contributions from the acceptor stretching band and we have restricted the band integration to the doublet itself. For TFIP, a strong dimer band is seen at 3550 cm^{-1} and a weaker band near 3445 cm^{-1} may be attributable to larger clusters, since it grows more than linearly with pressure.

Based on the B3LYP band strenghts of the most stable dimer conformers, approximate lower bounds of the dimerization constants are obtained and given in Table 4. Best estimates are 2−3 times higher due to the expected difference between thermal and zero point band strengths.[41] The observed trend, namely, a decreasing tendency for dimerization with increasing fluorination, should be reliable. For IP, the spectroscopic result for $K_{c,2}$ may be compared to an extrapolated value of ≈3 dm^3/mol for the second virial coefficient at 298 K,[42] which is most likely an overestimate due to wall effects and nonbonded contributions.[18] Interestingly, results for $K_{c,2}$ in CCl_4 solution[6] are also in good agreement with our gas-phase results (see Table 4), thus indicating that the influence of the solvent is relatively small in this case. In particular, a $K_{c,2}$ ratio between IP and HFIP of about 7 is found in CCl_4 solvent and in the gas phase. Using the estimated $K_{p,2}$ values, a dimer fraction of 0.1% near saturation at 298 K can be derived for TFIP and HFIP, whereas the IP dimer fraction is about twice as high. This is too small

TABLE 4: Equilibrium Constants for Dimerization $K_{p,2} = p_D p^{\ominus}/p_M^2$ ($p^{\ominus} = 1$ bar) and $K_{c,2} = c_D/c_M^2$ (c in mol/L) at 298 K for the Three Alcohols from Different Methods

K	IP	TFIP	HFIP	method
$K_{p,2}$	≥0.020	≥0.008	≥0.003	gas, IR + $\bar{A}_{th}$
$K_{p,2}$	≈0.01			B3LYP, harmonic oscillator/rigid rotor
$K_{c,2}$/(L mol^{-1})	≥0.5	≥0.2	≥0.07	gas, IR + $\bar{A}_{th}$
$K_{c,2}$/(L mol^{-1})	≈1.6		≈0.25	in CCl_4, IR, $\bar{A}_{acc} = \bar{A}_{mon}$[6]
$K_{c,2}$/(L mol^{-1})	≤3			virial coefficient[42]

TABLE 5: Band Maxima of Associated ($\tilde{\nu}_{ass}$) and Free OH Stretching Bands ($\tilde{\nu}_{free}$) in the Liquid Phase of IP, TFIP, and HFIP (298 K)[a]

$\tilde{\nu}$	IP	TFIP	HFIP
$\tilde{\nu}_{ass}$	3349	3379	3439
	⟨−309⟩	⟨−274⟩	⟨−187⟩
$\tilde{\nu}_{free}$		3688	3632
		⟨+35⟩	⟨−35⟩
$\tilde{\nu}_{free}$		3629	3592
		⟨−8⟩	⟨−34⟩

[a] The wavenumber shift relative to the corresponding monomer OH band is given in brackets. For the association band, the most stable monomer conformation is chosen.

for a reliable detection of the monomer depletion. Furthermore, the hydrogen bond acceptor stretching band overlaps with the monomer absorption region.

We have also attempted to estimate $K_{p,2}$ for the dimerization process from a simple harmonic oscillator/rigid rotor model using the B3LYP results for the various isomers. For IP, summation over all dimer conformations and appropriate inclusion of degeneracies leads to $K_{p,2} \approx 0.01$ at 298 K (Table 4). Considering the crudeness of the harmonic approximation for intermolecular degrees of freedom, this is in reasonable agreement with the experimental value of $K_{p,2} = 0.02$ and underestimates it, as expected. For HFIP, $K_{p,2}$ is underestimated by a factor of about 6.

Clearly, the dimerization tendency decreases with increasing fluorination of the methyl groups in 2-propanol and the shoulders at low frequency observed for IP and TFIP indicate that this also applies to larger clusters. In contrast, the wavenumber shift from the monomer to the dimer donor OH-stretching band in the gas phase stays approximately constant near −100 cm^{-1}. Before turning to the more reliable supersonic jet spectra, a discussion of the IR spectra of the neat liquid alcohols is appropriate.

6. Hydrogen Bonding in Condensed Phase

Figures 1−3 show the transmission spectra of liquid films for the alcohols under investigation. ATR spectra have also been recorded, but they exhibit the well-known band shifts due to the dependence of the penetration depth on wavelength and refractive index dispersion.[34,43] These shifts are particularly pronounced for the broad association bands, where they reach up to 20 cm^{-1} even after correction for the trivial $1/\nu$ dependence of the penetration depth. Therefore, we will only discuss transmission spectra at this stage.

Table 5 contains the approximate band centers for the broad association bands observed in liquid films at 298 K. The shift to lower frequencies relative to the gas phase band center for the most stable conformer decreases from IP over TFIP to HFIP. This indicates that larger clusters become less strongly bound along the fluorination series. While the proton donor ability increases from IP to HFIP, the decreasing basicity of the acceptor molecule appears to limit the strength of the hydrogen bond in these alcohol clusters. Overall, the cooperativity of the hydrogen bond is apparently attenuated by fluorination. Part of this may also be related to the increased size of the CF_3 substituent.

On the high-frequency wing of the association band, close to the free monomer band position in the gas phase, several shoulders are visible for the fluorinated alcohols[6,7] (see Figures 2 and 3). For IP, such absorptions are very weak at room temperature and we refrain from giving band centers. In HFIP, the corresponding bands are much stronger. They are shifted to lower frequencies relative to the gas phase monomer band position. For TFIP, shoulders of intermediate size occur at higher and lower frequencies relative to the free gas phase monomer. We plan to study these absorptions in more detail as a function of temperature. They are due to OH groups which are not engaged in a hydrogen bond to another oxygen atom but may be loosely connected to a C−F bond of a neighboring molecule. Thus, the effective hydrogen bond chain length in the associated liquid appears to drop with increasing fluorination.

Comparison of the integrated OH band strength per molecule in the gas and liquid phase is possible under the assumption that the CH-stretching bands are not significantly affected by hydrogen bond aggregation. This is confirmed by B3LYP results for IP and to a lesser extent for TFIP, but in general, significant couplings may occur.[44] In the case of HFIP, the only remaining C−H bond is in fact quite sensitive to OH conformation and hydrogen bonding.[7] Nevertheless, the enhancement of the integrated absorption coefficient from the gas phase to the room-temperature liquid can be estimated around 38 for IP, 17 for TFIP, and ≈11 for HFIP. This is in line with a decreasing hydrogen bond strength in this sequence (by about 7% according to the relationship found by Iogansen[45]) and it also contributes to the relative increase in free OH absorptions upon fluorination. IR fundamental band strengths appear to be more sensitive to the details of hydrogen bonding than room-temperature frequency shifts.

7. Hydrogen Bonding in Supersonic Jets

Beyond these qualitative and semiquantitative observations about the effect of fluorination on hydrogen bonding in 2-propanol, it is desirable to collect low-temperature size-resolved spectroscopic information such as the OH stretching frequency as a function of cluster size. This is achieved by expanding dilute mixtures of the alcohols in helium through our pulsed slit jet source.[20] The bottom trace in Figures 1−3 shows typical spectra obtained from such expansions and Figure 5 illustrates the effect of successive dilution of the alcohol in the rare gas. Several general features can be noted. In the monomer OH-stretching region, the most stable conformer gives rise to a narrow, rather symmetric band. To lower wavenumbers, near the low-frequency end of the gas-phase dimer bands at around 3500 cm^{-1}, a relatively strong, narrow, slightly asymmetric band is found for each alcohol. Additional weak bands can be found in the spectral region where dimer and trimer absorptions are expected. Within the low-frequency slope of the OH association band observed in the liquid, the jet spectra

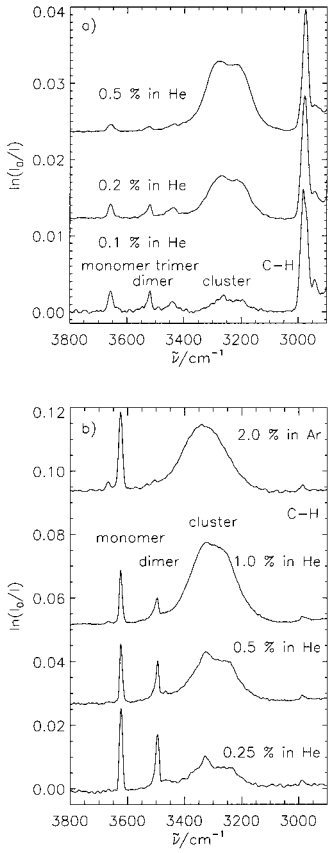

Figure 5. Effect of concentration on the spectra of (a) IP clusters (stagnation pressure 0.7−0.8 bar, resolution 6−8 cm^{-1}, scaled to similar C−H absorbance) and (b) HFIP clusters (stagnation pressures between 0.2 and 1.0 bar, resolution 4−8 cm^{-1}, scaled to similar C−H absorbance).

show a broad band. The appearance of this band is sensitive to the mixing ratio as well as to the inert gas used for the expansion and its pressure. At high dilution, the band has a weak doublet character. The high-frequency component appears to be in part due to oligomeric clusters. The remainder of the broad band structure must be due mainly to large, solid-, liquid-, or glasslike clusters.[28,46] In future work, we plan to compare these bands to bulk spectra of the condensed alcohols at different temperatures. Comparison to available literature data[7,9] suggests significant differences to the spectra of crystalline solids and comparison to time-resolved spectra[47] promises to provide detailed insights into the hydrogen bond structure and dynamics.

Turning to the bands near 3500 cm^{-1}, it is quite evident that they correspond to one or more of the most stable dimer conformations. They occur at the low-frequency end of the thermal dimer bands, where one would expect cold dimers to absorb. The wavenumber shifts predicted for the most stable conformers according to the B3LYP calculations agree quite closely (well within 10%) with the observed shifts (see Table 6). TFIP forms a possible exception, with at least two expected dimer bands due to the racemic character of the monomers. We shall therefore postpone the discussion of TFIP dimers until we have studied the spectra of a pure enantiomer. Obviously, the good agreement between harmonic B3LYP wavenumber shifts and experimental anharmonic band center displacements must be a consequence of substantial error compensation,[28,44] but we have confirmed this nearly perfect compensation for several aliphatic alcohols,[20] suggesting that it is quite robust. In the case of IP, we find nine enantiomeric pairs of stable dimer conformations in the B3LYP calculations. The six pairs which

TABLE 6: Dimer OH Stretching Wavenumber Shifts $\Delta\tilde{\nu}$(D − M) in the Gas Phase and in the Jet, Compared to Harmonic B3LYP Predictions $\Delta\omega$(D − M) for the Most Stable Conformers of IP and Its Fluorinated Homologues[a]

	IP	TFIP	HFIP
$\Delta\tilde{\nu}$(D − M)/cm^{-1} gas	−96	−103	−99
$\Delta\tilde{\nu}$(D − M)/cm^{-1} jet	−141	−126	−130
$\Delta\omega$(D − M)/cm^{-1} B3LYP	−145		−129
D_0^h/(kJ mol^{-1}) B3LYP	19		17
$\bar{A}$(D)/$\bar{A}$(M) B3LYP	38	17	11
$\bar{A}$(C)/$\bar{A}$(M) jet	60	50	20
$\bar{A}$(C)/$\bar{A}$(M) liquid	37	16	11

[a] Dimer dissociation energies D_0^h and intensity enhancements $\bar{A}$(X)/$\bar{A}$(M) per monomer due to dimerization (X = D) and large cluster formation (X = C) in the jet and in the liquid phase are also shown for the three compounds.

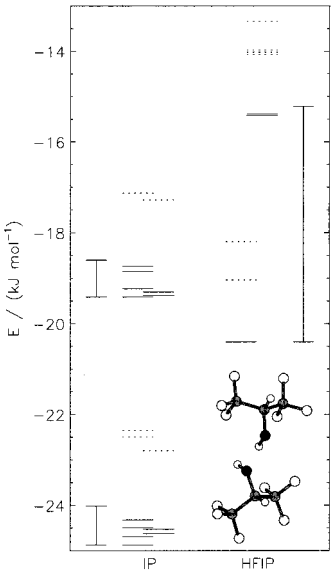

Figure 6. Comparison of binding energies *E* of the dimer conformations of IP and HFIP relative to the most stable monomer conformations at the B3LYP 6-31+G* level. For IP, both electronic (lower block around −24 kJ/mol) and harmonically zero-point energy corrected binding energies (upper block around −18 kJ/mol) are shown. For HFIP, only the electronic energies are given for clarity. Dimers with the donor molecule in the most stable conformation are drawn as full lines (6 for IP, 3 for HFIP), the others as dashed lines. Dimers with the acceptor molecule in the most stable conformation are drawn on the left, the others on the right side of the stack. To the very left and right, bars indicate the conformational energy difference in the monomer. The insert in the HFIP column shows the most stable HFIP dimer conformation ($(ap)^D$−$(ap)^A$), as predicted by the B3LYP calculation.

contain an $(sc)^D$ molecule fall within an energy window of 0.5−0.7 kJ/mol, which is about 2 kJ/mol below the narrow window of the three remaining dimers with $(ap)^D$ molecules (see Figure 6). The detailed sequence of conformers is quite sensitive to subtle details such as zero point energy contributions. Relative to the respective donor monomer, the wavenumber shifts are quite similar among the nine rotamers. Relative to the (sc) monomer band, the $(sc)^D$ dimers bunch at a harmonic wavenumber shift of −144 to −153 cm^{-1}, which is reasonably well separated from the −159 to −160 cm^{-1} shift predicted for the $(ap)^D$ dimers. Most likely, several of the six $(sc)^D$ dimer pairs contribute to the absorption band and this is confirmed by a significant dependence of the band maximum on expansion conditions. For comparison, ethanol dimer, which also has up to nine enantiomeric pairs of stable conformations, gives rise to three distinct OH stretching peaks.[20]

For HFIP, the situation is somewhat simpler, with the $(ap)^D-(ap)^A$ dimer being at least 1 kJ/mol more stable than the other eight diastereomeric conformers. Therefore, the low-temperature expansion may be dominated not only by a single monomer, but also by a single pair of enantiomeric dimer conformations. The predicted wavenumber shift of -129 cm^{-1} agrees perfectly with the observed shift of -130 cm^{-1}. However, there is the possibility that higher-lying conformers are frozen during the expansion. The rotational temperature of $\approx 10-20$ K is typically below the torsional or vibrational temperature. An estimate of the latter can be obtained for HFIP monomer from the known or calculated conformational equilibrium (vide supra). For the most dilute expansions (0.25−0.5% in He), the torsional temperature is found to be well below 100 K, whereas the spectrum for 2% in Ar (top trace in Figure 5b) corresponds to an effective torsional temperature around 160 ± 20 K. This suggests that the dimer population in the jet may indeed be dominated by $(ap)^D-(ap)^A$ conformations. Nevertheless, it is interesting to see that the energy gap to the next higher conformations ($(sc)^D-(ap)^A$) is less than one-half of the corresponding energy difference in the monomer. This indicates favorable secondary interactions which become available to the donor molecule in the (sc) conformation. In fact, relative to the constituent fragments, $(sc)^D$ dimers are more strongly bound by about 3−4 kJ/mol than $(ap)^D$ dimers. $(sc)^D$ dimers also have considerably larger dipole moments (3−5 D) than $(ap)^D$ dimers (1−2 D). Dipolar interactions between the monomers clearly play an important role. A lack of correlation of the dissociation energy with the intermolecular C−F···H−O distance indicates that direct hydrogen bonds to the fluorine atoms are less important. Independent of the mechanism, the results suggest that one can tune the (ap)−(sc) isomerization energetics in HFIP through a wide range by approaching another HFIP molecule. We plan to explore this effect in further experimental investigations.

Toward lower frequencies, there are additional, weaker bands visible in the spectra of all three compounds. With increasing fluorination, these bands loose intensity and approach the dimer band position. Tentatively and in analogy to the methanol case, we assign these bands to OH absorptions from molecular trimers in which the three hydrogen bonds form a ring. A reasonably systematic density functional study is currently restricted to the IP trimer, for which the B3LYP 6-31+G* calculation predicts a doublet of strong bands shifted between -200 and -225 cm^{-1} from the (sc) monomer and a much weaker component at lower frequency. The experimental band (Figure 1) is broad. Its maximum is shifted by -226 cm^{-1} from the corresponding monomer band. This is less than twice the dimer donor shift and indicates that sterical hindrance and associated ring strain counteract the usual cooperative enhancement observed for the trimer shift. For comparison, the donor band of the methanol dimer (Figure 7) is approximately midway between the monomer and trimer absorptions[20,48] and the donor band of HF dimer is even closer to that of the monomer than to that of the trimer.[28] In the case of HFIP, a very weak band near the low-frequency wing of the dimer band is the only available candidate for a trimer absorption. Such an assignment, or else the complete absence of a trimer band, would indicate a very pronounced destabilization of the ring trimer due to steric and polar interactions.

Bulky groups cannot avoid each other completely in a ring trimer, whereas this is easier for a ring tetramer in an up−down-up−down sequence. Therefore, and in analogy to the methanol case,[48] we propose that the sharp band which we find superimposed on the large cluster bands near 3300 cm^{-1} for IP and HFIP expansions at high dilution (see Figure 5) may be due to cyclic tetramers of these alcohols. This assignment is supported by similar structures in the jet spectra of other aliphatic alcohols,[20] but it remains to be confirmed by electronic structure calculations and possibly by size-selected spectroscopy.[49] Figure 7 illustrates the cluster size trends for methanol, IP, and HFIP based on this tentative assignment. Compared to methanol, IP exhibits a larger dimer shift, but the kink for $n = 3$ suggests steric hindrance. HFIP shows consistently smaller shifts, indicative of weaker interactions and in line with the findings for the liquid phase. To correlate these frequency shifts with hydrogen bond energies, reliable cluster dissociation energies would be required. In contrast to the elegant experimental methods available for very small[50] or aromatic clusters,[51] there is no general, accurate experimental technique available for the alcohol clusters under investigation. Also, the theoretical dissociation energies, calculated for the dimers (Table 6 and Figure 6) and in part for the trimers, remain quite uncertain due to the low levels of electronic structure calculations which have been applied. Therefore, we postpone a detailed discussion of hydrogen bond strengths in these systems. We note, however, that Iogansen's relationship[45] between the hydrogen bond energy and the XH stretching band strength enhancement is obeyed remarkably well by the B3LYP results. Using the harmonically corrected dissociation energy D_0^h as a measure of hydrogen bond strength and our double-harmonic estimate of the square root of the donor band strength $\bar{A}^{1/2}$, we find $D_0^h \approx b\Delta\bar{A}^{1/2}$ with b close to 1 kJ (km mol)$^{-1/2}$ for the most stable dimers. Inclusion of all calculated dimer conformations leads to a 10% larger value and more pronounced scatter of the data. Iogansen[45] found $b = 1.22$ kJ (km mol)$^{-1/2}$ in comparing thermal values of the hydrogen bond enthalpy and band strength over a wide range of hydrogen bonded liquids and solutions. The success of this simple relationship is remarkable but somewhat difficult to rationalize from a theoretical point of view.[45] At this stage, it can at least provide additional support for some of our B3LYP results.

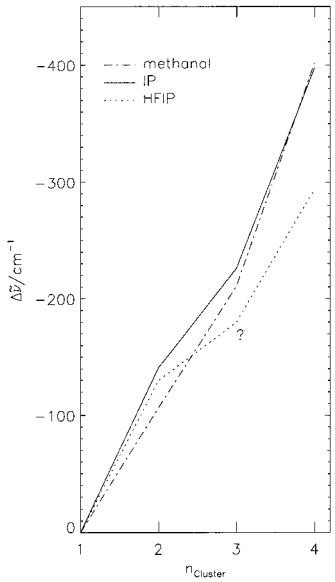

Figure 7. Hydrogen bond donor frequency shift as a function of cluster size for tentative band assignments, as discussed in the text. The dimer shift increases with methylation and decreases with fluorination, in line with the corresponding inductive effects on the hydrogen bond strength. The trimer shift is more sensitive to sterical and electronic hindrance. The tetramer shift is less affected by these constraints, resulting in a pronounced kink at $n = 3$.

Using the B3LYP intensity information, an estimate of the average cluster concentration in the region of the supersonic jet expansions which is probed by the FTIR beam becomes possible. For all three alcohols, we find monomer concentrations of the order of 10^{15} cm^{-3}. For IP, dimer concentrations around 2×10^{13} cm^{-3} and about 1 order of magnitude less trimers are found. For TFIP, the dimer concentration is around 10^{13} cm^{-3}. For HFIP, it reaches 7×10^{13} cm^{-3}. These values are averages over a 5-mm-diameter section near the nozzle, and peak concentrations might be higher.[20] They are comparable to or slightly higher than the ones obtained in recent CRD experiments,[48] but we can maintain these concentrations for much longer time periods due to the large buffer volume which we employ.

Similar to the procedure for the liquid-state spectra, intensity enhancements in large, cold clusters can be determined from the jet spectra under appropriate expansion conditions. Table 6 summarizes our findings, which are based on the assumption that the CH chromophore is much less affected by clustering and can therefore serve as a reference for the number concentration. As in the liquid phase, the enhancement factor drops with fluorination. Overall, it is about twice as large as in the room-temperature liquid. This is in line with thermal weakening of the hydrogen bond and with the observed decrease in band strength with increasing temperature.[41]

8. Conclusions and Outlook

In this study of hydrogen bonding in 2-propanol and its tri- and hexafluorinated derivatives, three simple techniques have proven to be very useful:

(i) A spectral difference technique has revealed spectroscopic details of the cluster traces which coexist with monomeric species in the equilibrium gas phase of such bulky alcohols.

(ii) A combination of rapid-scan FTIR and buffered, pulsed supersonic jet expansions has provided low temperature, size- and partly conformation-resolved monomer and cluster spectra for these compounds. This adds a new, powerful dimension to routine FTIR studies of hydrogen-bonded systems, beyond the well-established gas, liquid, solid, matrix, and solution techniques.[37]

(iii) Despite its methodical shortcomings, a simple harmonic 6-31+G* B3LYP computational approach has proven to be quite adequate for the interpretation of the spectroscopic results at the level at which they are currently available.

The most important findings may be summarized as follows:

Fluorination of the two methyl groups in 2-propanol inverts the conformational equilibria with respect to the O−H torsional degree of freedom. Intermolecular hydrogen bonding strongly affects the energetics in this torsional subspace. Cyclic trimer formation is disfavored, most likely due to unfavorable electrostatic and steric effects. On the other hand, the tendency for dimer formation is only moderately affected. Low-lying excited conformers can be expected to couple strongly to intramolecular excitations of the most stable (ap) conformation. Nearly pure, single conformation monomer/dimer expansions can be generated in the case of 1,1,1,3,3,3-hexafluoro-2-propanol (HFIP). Thus, HFIP and its dimer appear to be excellent prototypes for a systematic study of the isomerization and hydrogen bond dynamics and energetics. For the isomerization dynamics of HFIP monomer, this has already been noted before.[13] Ultimately, one should even be able to arrive at a deeper understanding of the exceptional solvent properties of bulk HFIP. We plan to investigate the energetics and dynamics of fluorinated 2-propanols in detail, using laser excitation and broad-band FTIR detection of the excited states as well as electronic structure and nuclear dynamics calculations.

Acknowledgment. We thank M. Kunzmann, U. Schmitt, and D. Tanke for extensive help and discussions and M. Quack for bringing refs 10 and 13, which we had overlooked, to our attention. Support from the Deutsche Forschungsgemeinschaft via SFB 357 (Molekulare Mechanismen unimolekularer Prozesse) and from the Fonds der Chemischen Industrie are gratefully acknowledged. Generous computational resources have been granted by the GWDG in Göttingen and by the John von Neumann Institute for Computing in Jülich.

References and Notes

(1) Seebach, D. *Angew. Chem., Int. Ed. Engl.* **1990**, *29*, 1320.
(2) Narita, M.; Honda, S. *Bull. Chem. Soc. Jpn.* **1988**, *61*, 281−284.
(3) Barbarich, T. J.; Rithner, C. D.; Miller, S. M.; Anderson, O. P.; Strauss, S. H. *J. Am. Chem. Soc.* **1999**, *121*, 4280−4281.
(4) Eger, E. I. *Anesthesiology* **1994**, *80*, 906−922.
(5) Murto, J.; Kivinen, A. *Suomen Kemistilehti B* **1967**, *40*, 14−18.
(6) Kivinen, A.; Murto, J. *Suomen Kemistilehti B* **1967**, *40*, 6−13.
(7) Murto, J.; Kivinen, A.; Viitala, R.; Hyömäki, J. *Spectrochim. Acta A* **1973**, *29*, 1121−1137.
(8) Barnes, A. J.; Hallam, H. E.; Jones, D. *Proc. R. Soc. London A* **1973**, *335*, 97−111.
(9) Murto, J.; Kivinen, A.; Edelmann, K.; Hassinen, E. *Spectrochim. Acta A* **1975**, *31*, 479−493.
(10) Hollenstein, H.; Quack, M.; Spirig, N. 1984, unpublished results. Spirig, N. Diploma Thesis, ETH Zürich, 1984.
(11) Durig, J. R.; Cox, F. O.; Groner, P.; van der Veken, B. J. *J. Phys. Chem.* **1987**, *91*, 3211−3218.
(12) Durig, J. R.; Larsen, R. A.; Cox, F. O.; van der Veken, B. J. *J. Mol. Struct.* **1988**, *172*, 183−201.
(13) Quack, M. *J. Chem. Soc., Faraday Discuss.* **1995**, *102*, 104−107.
(14) Howard, J. A. K.; Hoy, V. J.; O'Hagan, D.; Smith, G. T. *Tetrahedron* **1996**, *52*, 12613−12622.
(15) Biamonte, M. A.; Vasella, A. *Helv. Chim. Acta* **1998**, *81*, 695−717.
(16) Marstokk, K.-M.; Møllendal, H. *Acta Chem. Scand.* **1999**, *53*, 202−208.
(17) Kappes, M.; Leutwyler, S. Molecular Beams of Clusters. In *Atomic and Molecular Beam Methods*; Scoles, G., Ed.; Oxford University Press: Oxford, 1988; pp 380−140.
(18) Suhm, M. A. *Ber. Bunsen-Ges. Phys. Chem.* **1995**, *99*, 1159−1167.
(19) Quack, M.; Schmitt, U.; Suhm, M. A. *Chem. Phys. Lett.* **1997**, *269*, 29−38.
(20) Häber, T.; Schmitt, U.; Suhm, M. A. *Phys. Chem. Chem. Phys.* **1999**, *1*, 5573−5582.
(21) Amrein, A.; Quack, M.; Schmitt, U. *J. Phys. Chem.* **1988**, *92*, 5455−5466.
(22) Hartz, C. L.; Wofford, B. A.; McIntosh, A. L.; Meads, R. F.; Lucchese, R. R.; Bevan, J. W. *Ber. Bunsen-Ges. Phys. Chem.* **1995**, *99*, 447−456.
(23) Lovejoy, C. M.; Nesbitt, D. J. *J. Chem. Phys.* **1987**, *86*, 3151−3165.
(24) Rochester, C. H.; Symonds, J. R. *J. Chem. Soc., Faraday Trans. 1* **1973**, *69*, 1267.
(25) Frisch, M. J.; et al. *Gaussian98, Revision A.3*; Gaussian Inc.: Pittsburgh, PA, 1998.
(26) Maerker, C.; von Ragué Schleyer, P.; Liedl, K. R.; Ha, T.-K.; Quack, M.; Suhm, M. A. *J. Comput. Chem.* **1997**, *18*, 1695−1719.
(27) Hartke, B.; Schütz, M.; Werner, H.-J. Chem. Phys. **1998**, *239*, 561−572.
(28) Quack, M.; Suhm, M. A. Spectroscopy and Quantum Dynamics of Hydrogen Fluoride Clusters. In *Molecular Clusters*; Bowman, J. M., Bačić, Z., Eds.; JAI Press: London, 1998; Advances in Molecular Vibrations and Collision Dynamics, Vol. III, pp 205−248.
(29) Botschwina, P. *Chem. Phys.* **1983**, *81*, 73−85.
(30) Testa, B. *Principles of Organic Stereochemistry*; Decker: New York, 1979.
(31) van der Veken, B. J.; Coppens, P. *J. Mol. Struct.* **1986**, *142*, 359−362.
(32) Fang, H. L.; Compton, D. A. C. *J. Phys. Chem.* **1988**, *92*, 6518−6527.
(33) Singelenberg, F. A. J.; Lutz, E. T. G.; van der Maas, J. H. *Appl. Spectrosc.* **1986**, *40*, 1093−1098.
(34) Bertie, J. E.; Michaelian, K. H. *J. Chem. Phys.* **1998**, *109*, 6764−6771.
(35) Quack, M.; Suhm, M. A. *Chem. Phys. Lett.* **1995**, *234*, 71−76.

(36) Kreuzer, J.; Mecke, R. *Z. Phys. Chem.* **1941**, *49*, 309−323.
(37) Lüttke, W.; Mecke, R. *Z. Elektrochem.* **1949**, *53*, 241−249.
(38) Smith, F. A.; Creitz, E. C. *J. Res. Natl. Bur. Stand. (U.S.)* **1951**, *46*, 145−164.
(39) Coggeshall, N. D.; Saier, E. L. *J. Am. Chem. Soc.* **1951**, *73*, 5414−5418.
(40) Graja, A. *Acta Phys. Pol., A* **1976**, *49*, 603−610.
(41) Finch, J. N.; Lippincott, E. R. *J. Phys. Chem.* **1957**, *61*, 894−902.
(42) Kretschmer, C. B.; Wiebe, R. *J. Am. Chem. Soc.* **1954**, *76*, 2579−2583.
(43) Mirabella, Jr., Francis M., Principles, Theory, and Practice of Internal Reflection Spectroscopy. In *Internal Reflection Spectroscopy*; Mirabella, Jr., Francis M., Ed.; Marcel Dekker: New York, 1993; Practical Spectroscopy, Vol. 15, pp 17−52.
(44) Quack, M.; Willeke, M. *J. Chem. Phys.* **1999**, *110*, 11958−11970.
(45) Iogansen, A. V. *Spectrochim. Acta A* **1999**, *55*, 1585−1612.
(46) Bartell, L. S. *Chem. Rev.* **1986**, *86*, 492−505.
(47) Laenen, R.; Simeonidis, K. *Chem. Phys. Lett.* **1998**, *290*, 94−98.
(48) Provencal, R. A.; Paul, J. B.; Roth, K.; Chapo, C.; Casaes, R. N.; Saykally, R. J.; Tschumper, G. S.; Schaefer, H. F., III *J. Chem. Phys.* **1999**, *110*, 4258−4267.
(49) Buck, U. Vibrational spectroscopy of small size-selected clusters. In *Molecular Clusters*; Bowman, J. M.; Bačić, Z., Eds.; JAI Press: London, 1998; Advances in Molecular Vibrations and Collision Dynamics, Vol. 3, pp 127−161.
(50) Oudejans, L.; Miller, R. E. *J. Phys. Chem. A* **1997**, *101*, 7582−7592.
(51) Bürgi, T.; Droz, T.; Leutwyler, S. *Chem. Phys. Lett.* **1995**, *246*, 291−299.